

Dissolution dynamics of NaCl nanocrystal in liquid water

Yong Yang, Sheng Meng, L. F. Xu, and E. G. Wang

Institute of Physics, Chinese Academy of Sciences, Beijing 100080, China

Shiwu Gao

Department of Physics, Goteborg University, SE-41296, Goteborg, Sweden

and Institute of Physics, Chinese Academy of Sciences, Beijing 100080, China

(Received 28 February 2005; revised manuscript received 28 April 2005; published 22 July 2005)

The dissolution dynamics of a NaCl nanocrystal in liquid water was studied using molecular dynamics simulations. The dissolution process was found to start with a Cl^- ion at a corner site, followed by a Na^+ ion nearby. Both show directional preference in the dissolution path. An ion sequence with alternating charge, i.e., Cl^- , Na^+ , Cl^- , Na^+ , etc. was found to dominate the dissolution process. This image can be understood from the ionic hydration structures and the Coulomb interaction between the ions.

DOI: [10.1103/PhysRevE.72.012602](https://doi.org/10.1103/PhysRevE.72.012602)

PACS number(s): 64.75.+g, 61.46.+w, 82.20.Wt

Salt's process of dissolution and solvation in aqueous solutions represents a central prototype in surface physics, electrochemistry, biophysics, and environmental sciences. In our everyday experience, salt dissolves spontaneously in water, while the melting point of crystalline NaCl is as high as 1074 K [1]. These two observations immediately point to the atomic process related to water and NaCl, whose mechanism and dynamics have received much attention during the past few years [2–8]. Computer simulations based on empirical potentials and model systems have revealed the effect of water in dissociating a single NaCl molecule [2] and observed initial events for Cl^- dissolution in nanoclusters [3,4]. These studies provided insight into the initial stage of the dissolution process. However, a concise image of the dissolution process has not yet been established.

Here, we present a comprehensive study of salt dissolution, from its nanocrystal state, based on classical molecular dynamics simulations. The dissolution was found to start from a Cl^- ion at a corner site, followed by one of the Na^+ ions nearby. Both ions show a directional preference when leaving the crystal. An ion sequence with alternating charge was found to dissolve consecutively, maintaining charge neutrality or minimal charge separation on the crystal. This image is in contrast with the earlier one proposed by Ohtaki and collaborators [3,4]. Detailed analysis indicates that dissolution is accompanied with increase of water density around the ions, via a contraction of the first hydration shell of Cl^- and an increase of water coordination numbers of Na^+ . Our image can be understood from ion hydration dynamics and the electrostatic interactions of the hydrated systems.

The calculation was performed with classical molecular dynamics using AMBER 6 program package [9]. The simulation supercell, shown in Fig. 1(a), consists of 32 NaCl ion pairs in a cubic nanocrystal (with ~ 11.3 Å in each direction) surrounded by 625 water molecules in a liquid state with a density of ~ 1 g/cm³. Thus the interface between solid and liquid has six equivalent (100) faces (the six faces of the cubic nanocrystal are equivalent in $\langle 100 \rangle$ directions). The water–water interaction is described by the TIP3P model [10], while the ion–ion and ion–water interactions are given by the PARM94 force field in AMBER 6 [9]. The system was

prepared with an initial equilibration at ~ 300 K for 150 ps and then heated up to ~ 350 K for 100 ps to accelerate dissolution, before the production run started. The initial simulation box was 27.86 Å \times 27.88 Å \times 27.50 Å in size, which fluctuates within 0.5 Å during the NTP (canonical ensemble

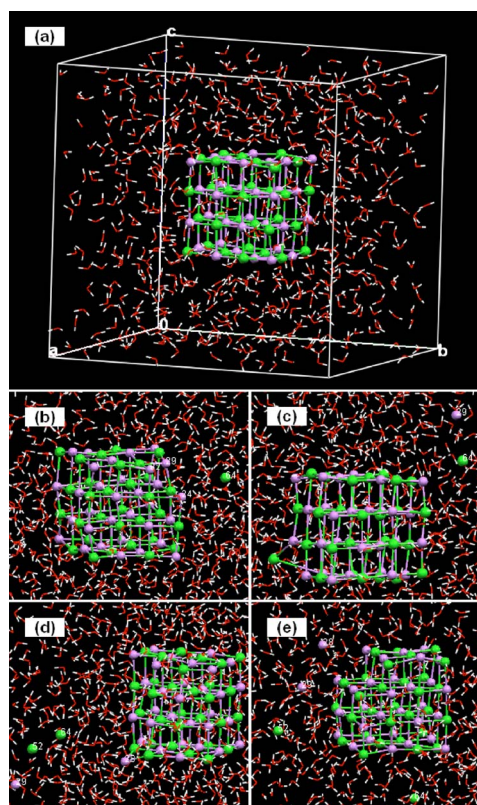


FIG. 1. (Color online) (a) Starting configuration used in our simulations. The Na^+ and Cl^- ions are represented by purple (smaller) and green (larger) balls, respectively. Water molecules are represented by sticks, white for hydrogen and red for oxygen, (b)–(e) MD snapshots at $t=241.635$ ps (b); 369.9 ps (c); 2013 ps (d); 2088 ps (e), showing a dissolution sequence of Cl^- , Na^+ , Cl^- , Na^+ , etc.

TABLE I. Geometries and binding energies for $\text{Na}^+(\text{H}_2\text{O})_n$ ($n=1-3$) and $\text{Cl}^-(\text{H}_2\text{O})_n$ ($n=1-3$) clusters, calculated by *ab initio* calculations and AMBER^a.

	<i>Ab initio</i> calculations			AMBER		
	O–Na (Å)	O–Cl (Å)	ΔE (kcal/mole)	O–Na (Å)	O–Cl (Å)	ΔE (kcal/mole)
$\text{Na}^+(\text{H}_2\text{O})$	2.228		–23.7	2.245		–22.90
$\text{Na}^+(\text{H}_2\text{O})_2$	2.253		–44.9	2.254		–44.25
$\text{Na}^+(\text{H}_2\text{O})_3$	2.282		–62.9	2.278		–62.60
$\text{Cl}^-(\text{H}_2\text{O})$		3.132	–13.7		3.247	–13.37
$\text{Cl}^-(\text{H}_2\text{O})_2$		3.214	–26.4		3.247	–26.25
$\text{Cl}^-(\text{H}_2\text{O})_3$		3.238	–39.3		3.265	–39.37

^aThe *ab initio* results of $\text{Na}^+(\text{H}_2\text{O})_n$ ($n=1-3$) were taken from Kim *et al.* (Ref. [15]), and those of $\text{Cl}^-(\text{H}_2\text{O})_n$ ($n=1-3$) were from Tobias *et al.* (Ref. [16]). The AMBER results were obtained from the present work. All the O–Na, O–Cl distances are averaged values.

with constant pressure) simulations. Periodic boundary condition is applied. Ewald summation [11,12] in energy and force calculation was truncated at 10 Å. A time step of 0.5 fs was used, and the OH vibrations were frozen using the SHAKE algorithm [13]. The trajectory was recorded every 15 fs at ~ 350 K. The temperature and pressure were controlled by the Berendsen’s thermostat and barostat [14], respectively, toward the target values of 350 K and 1 bar.

To test the validity of the model potentials used in AMBER, we first made a comparison between the available *ab initio* data [15,16] and the results given by AMBER for $\text{Na}^+(\text{H}_2\text{O})_n$ and $\text{Cl}^-(\text{H}_2\text{O})_n$ ($n=1,2$, and 3) clusters (Table I). Good agreement was found for both equilibrium distances and hydration energies. Extensive comparison was made between AMBER and the Vienna *ab initio* simulation package (VASP) [17], which gave comparable geometries and energetics for water adsorption on NaCl(100) surface (Table II).

Figure 2 shows the distances between the first dissolved $\text{Cl}^-(\text{Na}^+)$ and their neighboring ions in the NaCl crystal [panels (a) and (c)]. For convenience of discussion, we label the atoms in the crystal by a superscript ranging from 1 to 64 (1–32 for Na^+ and 33–64 for Cl^-). The eight corners of the crystal were occupied by 4 Na^+ and 4 Cl^- , each of which was bonded to three ions with opposite charges. The dissolution started with one of the corner ions, Cl^{64} , at ~ 232 ps, as seen by the increase of the bond length with the neighboring ions (Na^{24} , Na^{29} , and Na^{32}) [Figs. 1(b) and 2(a)]. At about 90 ps later, Na^{29} , which was originally bonded to Cl^{64} in the crystal, began to leave the corner. Continuation of the simulation

to more than 1 ns reveals a dissolution sequence, of Cl^- , Na^+ , Cl^- , Na^+ , etc., consecutively, which is schematically shown in Figs. 1(b)–1(e).

To examine the role of water in the dissolution process, the coordination number (CN) of water for the dissolved Cl^- and Na^+ ions are plotted as functions of time in Figs. 2(b) and 2(d). They are compared with two other corner ions, Cl^{36} and Na^{28} , which remain in the crystal during this simulation period. Here the CN is defined by counting the water molecules in a sphere within $r_{\text{Cl-O}} \leq 3.90$ Å and $r_{\text{Cl-H}} \leq 3$ Å for Cl^- , and $r_{\text{Na-O}} \leq 3.25$ Å for Na^+ , respectively. In aqueous solutions, these numbers correspond to the number of water molecules in the first hydration shell of the ions. Dissolution of the ions is correlated with a simultaneous increase in the CN of water. Detailed analysis indicates that the instantaneous force on the dissolving ions was mainly directed outward and increased slightly during the dissolution process [18]. This applies for both Na^+ and Cl^- ions.

Repeated simulations and analysis of different MD runs (with different starting configurations and particle velocities) [18] reveal the following features of the dissolution dynamics, which seem to be general for NaCl dissolution. First, the corner ions are more likely to dissolve first than the ions at other sites. This is reasonable because the corner ions have the fewest bonds with the crystal. It is also consistent with the fact that dissolution can hardly happen on a perfect NaCl (100) surface [19], as found from our classical and first-principle MD simulations and in Ref. [6]. Second, dissolution of the first Cl^- and Na^+ ions are accompanied with breaking two of the three Na^+-Cl^- bonds simultaneously,

TABLE II. Comparison between VASP and AMBER for adsorption of water monomer and 1 ML water overlayer on NaCl (100) surface. The HOH planes of water monomers were labeled by “flat” and “upright,” for two adsorbed configurations dominated by O– Na^+ attraction and H– Cl^- attraction, respectively. In the case of 1 ML adsorption, the HOH planes of water molecules are nearly parallel to the NaCl (100) surface.

Configuration	VASP			AMBER		
	O–Na (Å)	H–Cl (Å)	E_{ads} (eV/ H_2O)	O–Na (Å)	H–Cl (Å)	E_{ads} (eV/ H_2O)
Flat on Na^+	2.385	—	–0.401	2.408	—	–0.391
Upright on Cl^-	—	2.232	–0.174	—	2.250	–0.173
1 ML	2.434	—	–0.391	2.426	—	–0.406

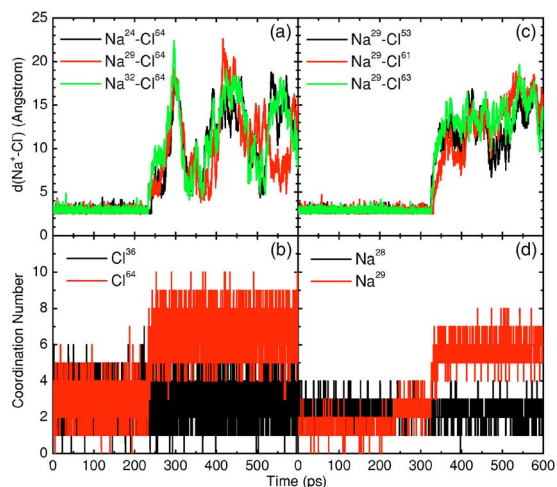


FIG. 2. (Color online) Evolution of the Na^+-Cl^- bond lengths and the water coordination number (CN) of the dissolved Cl^{64} (left panels) and Na^{29} (right panels). The CN of other two corner ions, Cl^{36} and Na^{28} , which do not dissolve during this period, are also shown.

while the third one is broken several picoseconds later, leading to directional preference in the dissolution trajectory. Third, the corner Cl^- is found to dissolve prior to corner Na^+ . This is mainly due to the different hydration structures and energetics between the two ions (see Table I and the following discussions).

From the trajectory analysis, the first two dissolved ions (Cl^{64} and Na^{29}) clearly show a directional preference in their dissolution path. Both slide along the $[11\bar{1}]$ direction first rather than the $[111]$ direction that one would intuitively expect [Fig. 3(a)]. Therefore the dissolved ions break two ionic bonds simultaneously while retaining the third bond through rotation around the bonded Na^+ (or Cl^- , when Na^+ is dissolved). This results from the crystalline structure. While a direct determination of the barriers would be difficult, we phenomenologically separate in Fig. 3 the dissolution barrier into two processes, the desorption of the ions from the crystal in vacuum (panel a) and the ionic hydration (panel b). Figure 3(a) shows that the energy barrier for removing the ions along $[11\bar{1}]$ has a nearly flat region, where the ions are

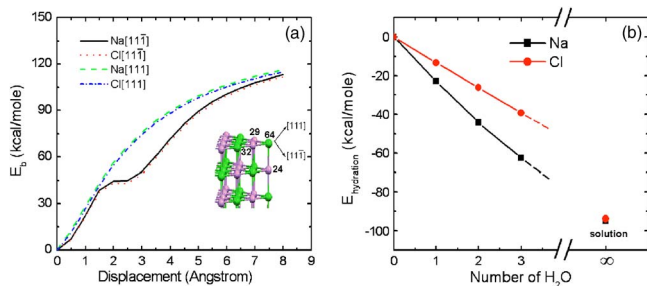


FIG. 3. (Color online) (a) Energy barrier for removing one $\text{Na}^+(\text{Cl}^-)$ from the corner site of a pure NaCl crystal into vacuum along the $[11\bar{1}]$ and $[111]$ directions, respectively; (b) hydration energy of Na^+ and Cl^- ions as a function of the number of water molecules, where the infinite number represents Na^+ and Cl^- ions in aqueous solutions.

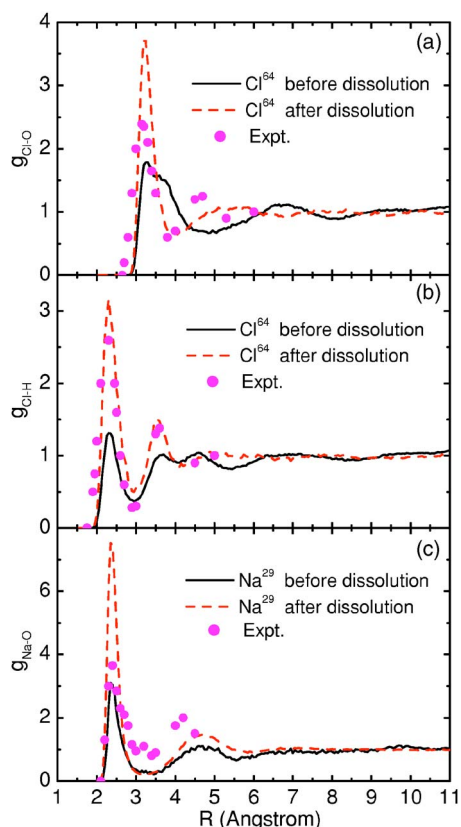


FIG. 4. (Color online). Radial distribution functions $g_{\text{Cl-O}}$, $g_{\text{Cl-H}}$, $g_{\text{Na-O}}$ for the two dissolved ions, Cl^{64} and Na^{29} , before and after dissolution. The time spans used in statistical analysis for Cl^{64} are 0–232.05 ps and 232.065–300 ps, and for Na^{29} are 300–324 ps and 324.015–600 ps, respectively. The experimental data ([22,23]) are shown by scattered dots.

displaced by 2–3 Å, and the ionic bonds were stretched to ~ 5 Å. The dissolution barrier is about 20 kcal/mole lower along $[11\bar{1}]$ than that in the $[111]$ direction. As a result, the dissolved ions strongly prefer to migrate along $[11\bar{1}]$ rather than $[111]$.

Why does Cl^- dissolve prior to Na^+ ? The hydration energies for Na^+ are larger both in small clusters [Fig. 3(b)] and in bulk water [-94.81 kcal/mole (average CN is 5.9) for Na^+ and -93.85 kcal/mole for Cl^- (average CN is 7.1)], so dissolution of Na^+ should be favored compared to Cl^- . Unexpectedly, Cl^- dissolves first into water. The answer lies in the barriers and kinetics of dissolution. From Fig. 3, we can see that the energy barrier for dissolving Na^+ is about 1 kcal/mole higher than that for Cl^- along either direction. The 1 kcal/mole energy difference is very small and is within the accuracy of model potentials. *Ab initio* calculations using VASP also give the same conclusion. Another important factor that contributes to the ion priority is the size of the hydration shells. As shown below, Cl^- has a much larger hydration shell and accommodates more water molecules in its first hydration shell compared to Na^+ . As a result, both configurational and rotational entropy would favor the hydration process of water around the Cl^- ion [20].

Figure 4 shows the radial distribution functions (RDF) of

water around the dissolved ions, averaged before and after the dissolution. In general, all the RDFs, $g_{\text{Cl-O}}$, $g_{\text{Cl-H}}$, and $g_{\text{Na-O}}$, change significantly upon dissolution. The first minimum of $g_{\text{Cl-O}}$, which defines the radius of the first Cl^- hydration shell [21], reduces from ~ 4.70 Å (crystal state) to ~ 3.90 Å (aqueous state), indicating the contraction of the first hydration shell and the strengthening of the ion-water interaction. From $g_{\text{Cl-O}}$ and $g_{\text{Cl-H}}$ we see that the oxygen shell of Cl^- resizes after dissolution whereas the hydrogen shell remains nearly the same size. In contrast, the size of the first hydration shell of Na^+ ions, as shown by the first minimum of $g_{\text{Na-O}}$ at ~ 3.25 Å, remains almost the same. Integration of the radial distribution function shows that the CN of water in the Na^+ hydration shell has increased from 2.6 to 5.7 upon dissolution, indicating a tightening of the hydration shell. Summarizing the RDF data, the dissolution dynamics involves mainly the contraction of the Cl^- hydration shell and a tightening of the Na^+ hydration shell.

When Cl^{64} leaves the crystal, the remaining nanocrystal becomes positively charged, and the three Na^+ ions close to Cl^{64} become new corner ions. The local ionic interactions lost equilibrium due to the absence of Cl^{64} . Aggregation of water molecules into the corner also increases the CN of the Na^+ ions by about one per ion. Therefore both the Coulomb repulsion between the three positive ions, Na^{24} , Na^{29} , Na^{32} , and the hydration force favor the Na^+ dissolution, as observed in the case of Na^{29} at $t \sim 324$ ps, shown in Fig. 2. This process recovers charge neutrality on the crystal. Longer MD runs, up to 1 ns, show a dissolution sequence with alternating charge, i.e., Cl^- , Na^+ , Cl^- , Na^+ , etc. shown in Figs. 1(b)–1(e). This sequence contrasts with the earlier studies [3,4], where the first ions that dissolved into water are all four Cl^- ions at the corner sites, while no Na^+ dissolution was ever observed. Our result is physically reasonable and can be understood simply from the electrostatic interactions between the dis-

solved ion and the nanocrystal. Removal of an anion from a crystal with a positive charge of 1–3 e is obviously unfavorable.

To compare with experiments, the radial distribution functions for the dissolved ions in solution state are comparable with the experimental data [22,23], as shown in Fig. 4. The peak positions of all RDFs, $g_{\text{Cl-O}}$, $g_{\text{Cl-H}}$, and $g_{\text{Na-O}}$, agree well with experiments, although the peaks observed in experiments are slightly broader. This difference is attributable to the dynamical broadening and quantum nature of the hydrogen dynamics of water molecules [24]. In addition, the calculated diffusion coefficients are also comparable with experimental data. During the dissolution process, ions diffuse slowly before getting fully hydrated in solution. The diffusion coefficient of Cl^- is $1.26 \times 10^{-9} \text{ m}^2 \text{ s}^{-1}$, compared to $2.25 \times 10^{-9} \text{ m}^2 \text{ s}^{-1}$ in solution (350 K). The latter is comparable with the experimental value of $2.032 \times 10^{-9} \text{ m}^2 \text{ s}^{-1}$ at 298 K [1].

In conclusion, we studied the dissolution dynamics of nanocrystalline NaCl in water through molecular dynamics simulations. The dissolution process has been captured by the first few events of dissolution together with the ion sequence. Bulk salt is thought to split into nanocrystals at defects, in the following dissolution process: Ions at the corner dissolve first along the $[11\bar{1}]$ directions. The other ions follow a dissolution sequence of Cl^- , Na^+ , Cl^- , Na^+ , etc., starting from the corner and edge sites. Ion dissolution is accompanied by dynamical transformation of hydration shells and instantaneous local density fluctuations of water molecules. These results, obtained on this model system, have general implications in the ionic processes at the solid-liquid interfaces.

The work was supported by the MOST and NSF of China. S.W. Gao acknowledges support from Chinese Academy of Science via the 100-Talent Plan.

-
- [1] *CRC Handbook of Chemistry and Physics*, 77th ed., edited by D. R. Lide (CRC, Boca Raton, FL, 1996).
- [2] P. L. Geissler *et al.*, *J. Phys. Chem. B* **103**, 3706 (1999); J. Martí *et al.*, *J. Chem. Phys.* **113**, 1154 (2000); J. Martí *et al.*, *Chem. Phys. Lett.* **328**, 169 (2000).
- [3] H. Ohtaki *et al.*, *Pure Appl. Chem.* **60**, 1321 (1988).
- [4] H. Ohtaki and N. Fukushima, *Pure Appl. Chem.* **61**, 179 (1989).
- [5] D. Zahn, *Phys. Rev. Lett.* **92**, 040801 (2004).
- [6] E. Oyen and R. Hentschke, *Langmuir* **18**, 547 (2002).
- [7] P. Jungwirth, *J. Phys. Chem. A* **104**, 145 (2000).
- [8] E. M. Knipping *et al.*, *Science* **288**, 301 (2000).
- [9] D. A. Case, D. A. Pearlman, J. W. Caldwell, *et al.*, AMBER 6, University of California, San Francisco, 1999.
- [10] W. L. Jorgensen *et al.*, *J. Chem. Phys.* **79**, 926 (1983).
- [11] T. Darden, D. York, and L. Pedersen, *J. Chem. Phys.* **98**, 10089 (1993).
- [12] U. Essmann *et al.*, *J. Chem. Phys.* **103**, 8577 (1995).
- [13] J. P. Ryckaert *et al.*, *J. Comput. Phys.* **23**, 327 (1977).
- [14] H. J. C. Berendsen *et al.*, *J. Chem. Phys.* **81**, 3684 (1984).
- [15] J. Kim *et al.*, *J. Chem. Phys.* **102**, 839 (1995).
- [16] D. J. Tobias, P. Jungwirth, and M. Parrinello, *J. Chem. Phys.* **114**, 7036 (2001).
- [17] G. Kresse and J. Hafner, *Phys. Rev. B* **47**, 558 (1993); **49**, 14251 (1994); G. Kresse and J. Furthmüller, *Comput. Mater. Sci.* **6**, 15 (1996); *Phys. Rev. B* **54**, 11169 (1996).
- [18] Y. Yang *et al.* (to be published).
- [19] B. J. Finlayson-Pitts (private communication).
- [20] Our simulations reveal that the Cl^- dissolution is due to the water reorganization (mainly through the *rotations* of H atoms) in the first hydration shell, while the Na^+ dissolution requires the *translation motions* of water molecules from the outer hydration shell to the first. Therefore the water molecules around corner Cl^- have a better chance to approach the ion and enhance the ion-water interactions.
- [21] S. B. Zhu and G. W. Robinson, *J. Chem. Phys.* **97**, 4336 (1992).
- [22] N. T. Skipper and G. W. Neilson, *J. Phys.: Condens. Matter* **1**, 4141 (1989).
- [23] D. H. Powell *et al.*, *J. Phys.: Condens. Matter* **5**, 5723 (1993).
- [24] M. E. Tuckerman *et al.*, *Nature (London)* **417**, 925 (2002).